ISSN 0036-0244, Russian Journal of Physical Chemistry A, 2019, Vol. 93, No. 11, pp. 2123–2130. © Pleiades Publishing, Ltd., 2019.
Russian Text © The Author(s), 2019, published in Zhurnal Fizicheskoi Khimii, 2019, Vol. 93, No. 11, pp. 1644–1651.

ON THE 90th ANNIVERSARY OF THE DEPARTMENT OF CHEMISTRY OF THE LOMONOSOV MOSCOW STATE UNIVERSITY

Thermal Stability of 4-*tert*-Butyl Diphenyl Oxide

V. A. Shakun[a],*, T. N. Nesterova[a], S. V. Tarazanov[b], and S. A. Spiridonov[a]
[a] *Samara State Technical University, Samara, 443100 Russia*
[b] *All-Russian Research Institute of Oil Refining, Moscow, 111116 Russia*
**e-mail: ShakyH@mail.ru*

Received February 11, 2019; revised February 11, 2019; accepted May 14, 2019

Abstract—In the temperature range of 703–763 K, the thermal stability of 4-*tert*-butyl diphenyl oxide (4-TBDPO) has been studied, the components of the thermolysis reaction mass have been identified, a kinetic model of the process has been proposed, and the rate constants and parameters of the Arrhenius equation for all reactions under consideration have been calculated. The predominant role of isomerization transformations of 4-TBDPO has been found. A mechanism for the radical isomerization of the *tert*-butyl substituent has been proposed.

Keywords: 4-*tert*-butyl diphenyl oxide, thermal stability, thermal degradation, isomerization, kinetics
DOI: 10.1134/S0036024419110244

Diphenyl oxide (DPO) and its alkyl derivatives are of scientific interest and of great practical importance in the development of modern industry.

It is well known that DPO mixed with biphenyl is used as a high-temperature coolant [1, 2]. Based on DPO derivatives, polymers are created that possess unique mechanical and optical properties [3]; some of alkyl DPOs, including those containing C_4 substituents, exhibit the properties of liquid crystals [4].

However, information on the thermal stability of diphenyl oxide and its derivatives is limited. The most extensive studies [5, 6] have been devoted to determining the initial temperatures and minimum decomposition energies of alkyl aromatic esters in order to determine promising hydraulic fluids and lubricants.

Recently, interest has increased in the study of the thermal stability of alkylbenzenes in the production of promising fuels. Among other compounds, much attention is paid to butylbenzenes [7–10] as model structures. These studies are united by the fact that in reactors of various materials (gold, steel, and glass) in the temperature range 500–800 K, the decay of *n*-butylbenzene (NBB) and *tert*-butylbenzene (TBB) by the radical mechanism was accompanied by the formation of *sec*-butylbenzene (SBB) and isobutylbenzene (IBB), respectively.

In this work, 4-*tert*-butyl diphenyl oxide (4-TBDPO) was chosen as the object of study as a compound that combines the properties of alkylarenes and aromatic ethers. We have carried out an analysis of the mutual transformations of thermolysis products, and it has been shown that the isomerization of 4-TBDPO plays a decisive role in the decomposition process.

This information is of great importance in the research and development of thermostable and heat-resistant polymers. It is known [11] that aromatic polyethers have high thermal stability and heat resistance, and the presence of an alkyl substituent in the core gives the polymer additional properties; for example, an increased glass transition temperature. Polyphenylene oxides and their alkyl derivatives are used at temperatures up to 623 K; therefore, the results obtained are relevant for developing understandings of their properties.

EXPERIMENTAL

Starting materials. 4-TBDPO was synthesized, isolated, and purified according to the known procedure [12]. The concentration of the main substance was 99.93 wt % according to GLC.

Procedure for studying 4-TBDPO thermolysis. Thermolysis was studied in the gas phase in glass capillaries (l = 23–25 mm; d_n = 0.95–1.05 mm) made of Pyrex, in which the test substance was placed. The capillary was flushed with helium (purity 99.999%) and sealed. The degree of filling was 25–27% of the volume, which corresponded to a substance mass of 0.8–1.0 mg. Samples were weighted on an Shimadzu AUW 120D analytical balance with an accuracy of 10^{-4} g. The capillary with the substance was thermostatted in a laboratory pyrolysis furnace, which ensured the accuracy of maintaining the temperature

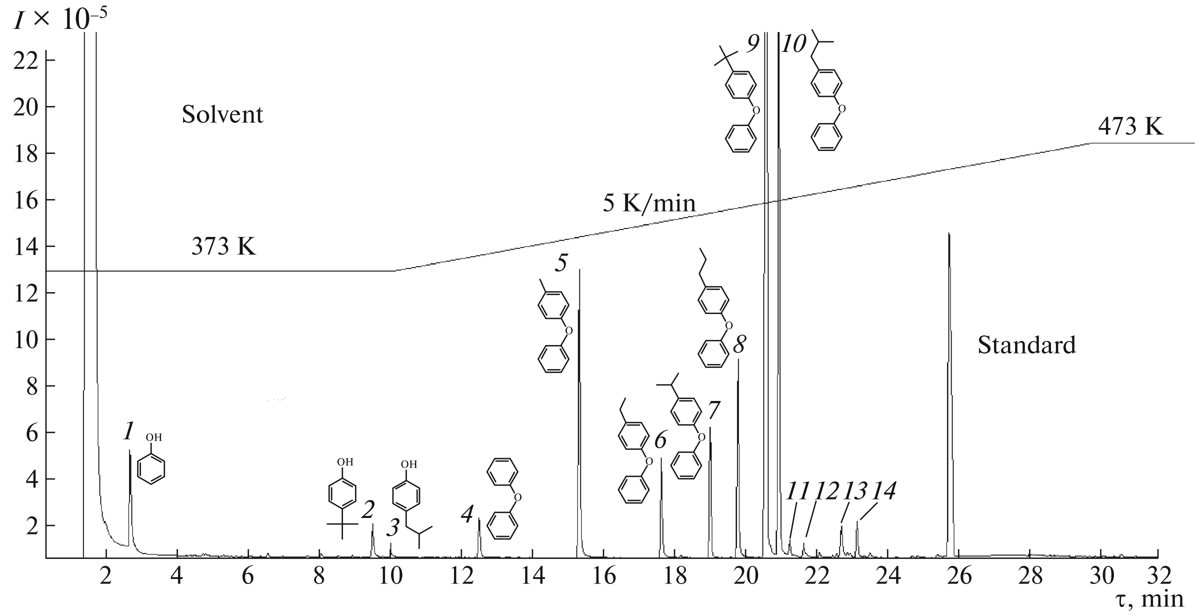

Fig. 1. Chromatogram of the mixture of products of the 4-TBDPO thermal decomposition ($T = 728$ K, $t_{\text{cont}} = 40$ min): (*1*) phenol, (*2*) 4-*tert*-butylphenol (4-TBP), (*3*) 4-isobutylphenol (4-IBP), (*4*) diphenyl oxide (DPO), (*5*) 4-methyldiphenyl oxide (4-MeDPO), (*6*) 4-ethyl diphenyl oxide (4-EDPO), (*7*) 4-isopropyl diphenyl oxide (4-IPDPO), (*8*) 4-*n*-propyl diphenyl oxide (4-NPDPO), (*9*) 4-*tert*-butyl diphenyl oxide (4-TBDPO), (*10*) 4-isobutyl diphenyl oxide (4-IBDPO), (*11–14*) undefined components X_1–X_4.

in the isothermal zone to be ±1 K; the device was previously reported [13]. The time to reach the isothermal mode after the capillary was placed in the furnace did not exceed 60 s. The pyrolysis process was completed by quenching in a tube cooled to –15°C. The thermal stability of 4-TBDPO was studied in the temperature range 703–763 K with a step of 5 K. The conversion of 4-TBDPO did not exceed 25%; the number of moles in the process increased by no more than 5%.

Analysis and identification of components of the thermolysis reaction mixture. GLC was used as the main method for the analysis of reaction mixtures. The analysis was performed on a Crystal 2000 M chromatograph equipped with a SE-30 quartz capillary column (60 m × 250 μm × 0.25 μm). The temperature profile of the analysis is shown in the chromatogram (Fig. 1). The temperature of the evaporator was 250°C, while that of the detector was 280°C.

A quantitative analysis of the composition of the reaction mixture was performed by the internal standard method using $n\text{-}C_{20}H_{42}$ as the internal standard (98.0 wt % according to GLC), the value of the calibration coefficient with respect to 4-TBDPO was 0.9625 ± 0.067.

Identification of the components of the mixtures included directed chemical synthesis and chromatography-mass spectrometric analysis (70 eV) performed on an Agilent 6850 gas chromatograph equipped with an HP-5MS Agilent 19091S-433E capillary column (30 m × 0.25 mm × 0.25 μm) and an Agilent 5975C VL MSD mass-selective detector. The reaction products were identified using the rules and approaches described by Lebedev [14], Pretsch, Buhlmann, and Affolter [15] as well as data from the NIST 2017 library [16].

The identity of 4-IBDPO (*10*) was approved by the synthesis of its sample. 4-IBDPO was obtained by the Würz–Fittig reaction from 4-bromodiphenyl ether and isobutyl bromide on sodium chips in *n*-hexane at room temperature. 4-Bromodiphenyl ether was obtained by bromination of DPO with liquid bromine at room temperature; the DPO/Br_2 ratio was 20/1 mol/mol. The retention time of synthesized 4-IBDPO corresponded to component (*10*) in Fig. 1. Overlaying chromatograms are not given because this reduces the information content.

Alkyl DPOs have no positional isomers and were identified in accordance with the rules for the determination of alkyl aromatic structures [14, 15]. 4-TBP was identified by comparing its retention time with the standard sample. 4-IBP was identified by comparing the retention times and mass spectra of component (*3*) and 4-*n*-butylphenol (>98 wt % according to GLC), which was added to the mixture to be analyzed.

In the reaction mass, under conditions of deep conversion, trace amounts (>0.1 mol %) of isopropylbenzene and *tert*-butylbenzene were also observed. The concentration of unidentified components X_1–X_4

Table 1. Characterization of mass spectra of the reaction mass of thermolysis of 4-TBDPO

Compound	Mass spectrum 70 eV (m/z, intensity, rel. %)
Phenol	94 (M^+, 100), 66 (46), 39 (43)
4-TBP	150 (M^+, 23), 135 (100), 107 (42), 91 (10), 77 (10)
4-IBP	150 (M^+, 14), 107 (100), 91 (1), 77 (12)
DPO	170 (M^+, 45), 141 (72), 115 (26), 94 (4), 77 (60)
4-MeDPO	184 (M^+, 100), 169 (4), 141 (15), 91 (100), 77 (50)
4-EDPO	198 (M^+, 58), 183 (100), 169 (5), 153 (10), 105 (16), 91 (15), 77 (57)
4-IPDPO	212(M^+, 37), 197 (100), 178 (4), 169 (2), 119 (6), 104 (14), 91 (36), 77 (38)
4-NPDPO	212(M^+, 32), 183 (100), 165 (1), 153 (8), 107 (8), 91 (6), 77 (35)
4-TBDPO	226 (M^+, 31), 211 (100), 183 (6), 171 (1), 165 (2), 91 (8), 77 (12)
4-IBDPO	226 (M^+, 20), 183 (100), 165 (1), 115 (5), 107 (8), 91 (4), 77 (22)
X_1	224 (M^+, 100), 209 (22), 194 (4), 181 (7), 169 (3), 153 (10), 147 (5), 131 (92), 116 (72), 115 (58), 107 (14), 91 (48), 77 (84), 65 (13), 51 (52)
X_2	210 (M^+, 100), 195 (3), 184 (2), 181 (4), 165 (10), 152 (6), 141 (4), 133 (8), 117 (100), 115 (80), 103 (16), 91 (24), 77 (68), 65 (16), 51 (48)
X_3	224 (M^+, 100), 209 (7), 194 (4), 183 (5), 181 (6), 165 (5), 153 (4), 147 (6), 131 (50), 116 (68), 115 (64), 107 (5), 91 (50), 77 (72), 65 (20), 51 (44)
X_4	224 (M^+, 26), 209 (100), 194 (2), 181 (40), 169 (20), 152 (6), 139 (14), 126 (1), 115 (5), 104 (2), 98 (3), 90 (18), 76 (6), 63 (5), 51 (2)

Table 2. Change in concentrations of components of reaction mass of 4-TBDPO thermolysis at 728 K

Time, min	Molar concentration of components, mol %									
	phenol	4-TBP	4-IBP	DPO	4-MeDPO	4-EDPO	4-IPDPO	4-NPDPO	4-TBDPO	4-IBDPO
0.0	0.00	0.00	0.00	0.00	0.00	0.00	0.00	0.00	100.00	0.00
2.0	0.04	0.03	0.00	0.05	0.04	0.00	0.03	0.00	99.16	0.65
5.0	0.09	0.06	0.01	0.10	0.10	0.00	0.09	0.01	97.93	1.61
7.0	0.19	0.13	0.02	0.18	0.30	0.03	0.28	0.05	95.44	3.38
10.0	0.10	0.10	0.01	0.16	0.27	0.02	0.25	0.04	95.60	3.45
15.0	0.30	0.19	0.02	0.24	0.43	0.07	0.49	0.10	92.34	5.82
20.0	0.53	0.25	0.03	0.28	0.77	0.09	0.63	0.24	91.12	6.06
25.0	0.75	0.31	0.03	0.35	1.13	0.16	0.93	0.50	87.87	7.97
30.0	1.11	0.37	0.05	0.42	1.74	0.36	1.08	0.75	85.48	8.64
32.5	1.30	0.41	0.07	0.45	1.88	0.46	1.26	0.97	84.28	8.92
35.0	1.39	0.45	0.07	0.51	2.16	0.53	1.31	1.09	83.35	9.14
40.0	1.60	0.54	0.11	0.58	2.94	0.76	1.41	1.44	81.00	9.62
45.0	1.89	0.56	0.11	0.63	3.47	1.04	1.68	1.73	78.84	10.05
50.0	2.52	0.66	0.12	0.76	4.25	1.51	1.74	2.27	75.52	10.65

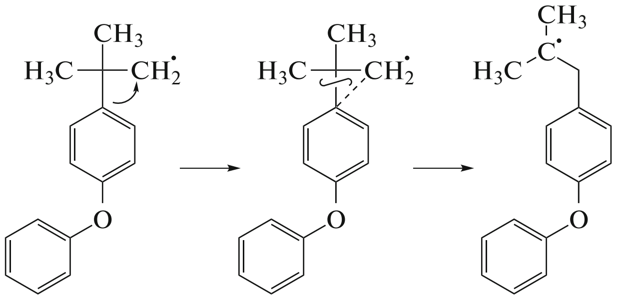

Fig. 2. Possible mechanism of isomerization of 4-TBDPO.

did not exceed 0.5 mol % in the most severe experimental conditions. When constructing the kinetic decay model, IPB, TBB, and components X_1–X_4 were not included in the processing.

The characteristics of the mass spectra of the components are given in Table 1.

RESULTS AND DISCUSSION

Possible Mechanism of Radical Isomerization of 4-TBDPO

Table 2 shows the change in the concentrations of the components of the reaction mixture at $T = 728$ K as a function of time.

Our analysis of the experimental data presented showed that during the thermolysis of 4-TBDPO, the isomerization of the *tert*-butyl substituent occurs most readily to form 4-IBDPO. For example, at 728 K and a contact time of 10 min, the concentration of 4-IBDPO is 3.45 mol % when the degree of conversion of 4-TBDPO is 4.40 mol %, i.e., the selectivity of the formation of 4-IBDPO was 78%. In general, under the experimental conditions, with the conversion of 4-TBDPO equal to 0–10%, the selectivity for the formation of 4-TBDPO is 70–80%. The destruction of 4-TBDPO is manifested to a much lesser extent and contributes to the formation of 4-TBP, phenol, and DPO as a result of the cleavage of the C_{Ar}–C_{quater} and C_{Ar}–O bonds. In this case, the decomposition practically has no effect on the alkyl substituent, since the concentration of 4-MeDPO and 4-IPDPO, for example, has an adequate relationship only with 4-IBDPO.

This direction of decay looks rather unexpected. Of particular interest is the fact that in the thermolysis products of 4-TBDPO, regardless of temperature or contact time (within the study conditions), no traces of 4-*n*-butyl DPO and 4-*sec*-butyl DPO were found. Obviously, this results from the mechanism of conversion of the *tert*-butyl substituent. Presumably, isomerization, which promotes the conversion of the *tert*-butyl substituent exclusively to *iso*-butyl, can occur through the formation of a three-membered ring between C_{prim} of the *tert*-butyl substituent and C_{Ar} of the aromatic nucleus (Fig. 2).

The above mechanism adequately explains why secondary and normal butylarenes are absent in the products of the 4-TBDPO thermolysis.

A similar result was obtained in the course of the thermolysis of 4-TBP [13]. The data obtained for 4-TBDPO and 4-TBP suggest the general nature of

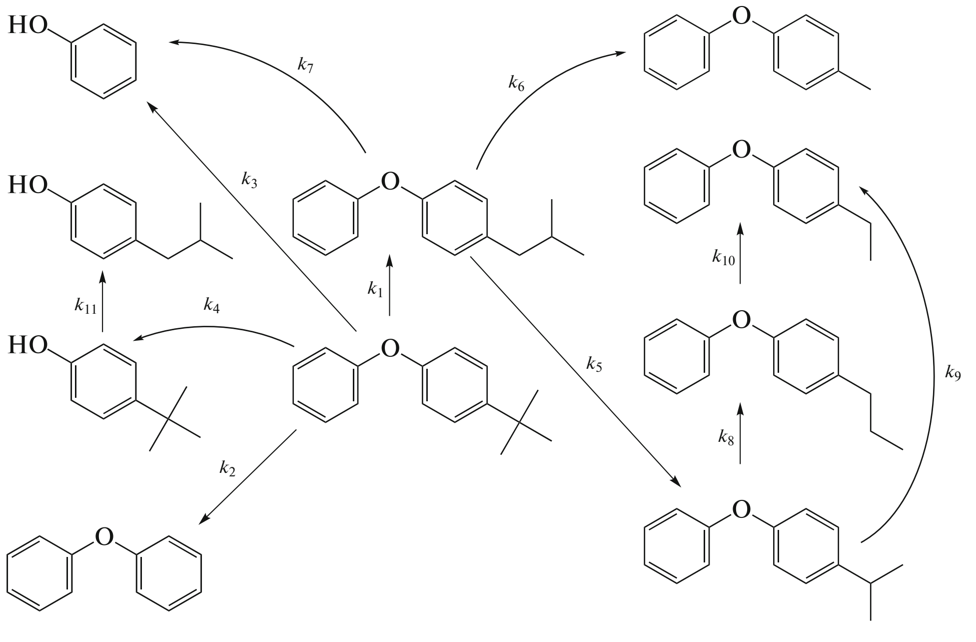

Fig. 3. Scheme of transformations during thermolysis of 4-TBDPO.

Table 3. Values of rate constants ($k_i \times 10^5$, s^{-1}) for transformations accompanying thermolysis of 4-TBDPO in the range 703–763 K

T, K	k_1	k_2	k_3	k_4	k_5	k_6	k_7	k_8	k_9	k_{10}	k_{11}
703	2.16	0.07	0.04	0.06	8.54	6.12	2.32	27.37	4.85	8.01	3.82
708	3.26	0.11	0.06	0.10	10.44	8.02	3.51	37.59	7.36	10.44	5.29
713	3.92	0.15	0.09	0.13	13.90	11.08	5.02	43.98	8.57	11.68	6.82
718	5.21	0.21	0.11	0.18	19.56	14.68	6.59	62.38	13.67	18.65	8.99
723	5.52	0.21	0.12	0.20	20.90	16.02	7.82	72.56	17.68	20.19	9.92
728	8.19	0.28	0.16	0.28	25.20	19.76	9.66	104.18	24.88	30.73	13.18
733	13.63	0.56	0.30	0.46	48.55	35.27	16.39	129.98	33.48	43.24	19.42
738	17.02	0.77	0.42	0.63	65.20	46.86	22.02	164.91	44.76	56.79	24.92
743	19.83	0.89	0.47	0.67	75.85	52.11	25.35	179.88	55.18	76.26	27.18
748	29.84	1.44	0.78	1.15	116.20	81.80	39.30	278.71	84.85	103.73	40.65
753	32.25	1.81	0.95	1.35	167.55	101.32	48.39	291.40	89.68	108.56	42.18
758	49.47	2.64	1.43	2.06	203.96	140.71	69.07	437.01	146.91	173.64	70.70
763	62.39	3.25	1.97	2.80	277.93	205.26	93.66	537.93	175.68	208.72	93.18

the radical isomerization of the *tert*-butyl substituent associated with various substituted arenes.

Development of Kinetic Model of 4-TBDPO Thermolysis

When developing a kinetic model of thermolysis of 4-TBDPO from a number of theoretically possible transformations in the system under study, a number of transformations of the greatest significance were identified (Fig. 3).

Obviously, during thermolysis, the reactions shown in the scheme (Fig. 3) proceed in several stages. It is also known that in the course of radical chain processes, the presence of free radicals provide no hindrances to implement monomolecular reactions [17]. Therefore, we assumed that all reactions selected for kinetic analysis are monomolecular. Accordingly, the rate constants indicated in the reaction scheme are a combination of rate constants of all stages of the reaction. The values of the rate constants of individual transformations were calculated in accordance with the following algorithm.

(i) For all reaction products, the actual rates of concentration change ($r_{i,\,\mathrm{exp}}$) were calculated, that is we calculated the differential from $C_{i,\,\mathrm{exp}} = f(\tau)$.

(ii) Rates ($r_{i,\,\mathrm{exp}}$) of the accumulation of products were calculated taking into account 38 most likely reactions according to Eq. (1):

$$r_{i,\mathrm{calc}} = \sum (k_j C_j). \tag{1}$$

(iii) By processing the dependencies obtained in (i) and (ii) combined with the optimization criterion (2)

$$\sum_n (r_{i,\mathrm{exp}} - r_{i,\mathrm{calc}})^2 \tag{2}$$

(where n is the number of measurements), we excluded insignificant reactions and calculated the rate constants k_j (Table 3). The error in determining the values of the rate constants was <10%.

(iv) Using the rate constants given in Table 3, the calculated values of the concentrations of 4-TBDPO thermolysis products were obtained by the Runge–Kutta method.

(v) Over the entire range of temperatures studied, the adequacy of the proposed model was tested by mathematical statistics methods using the Pearson criterion, the value of which exceeded 0.99, and the Fisher criterion, the calculated value of which at a significance level of 0.05 was many times higher than the tabulated value.

Figure 3 shows that the rate constant k_1 for the isomerization 4-TBDPO → 4-IBDPO is an order of magnitude higher than the rate constants of destructive processes (k_2–k_4) affecting the *tert*-butyl substituent and the C_{Ar}–O and C_{Ar}–C_{quater} bonds. In particular, at 728 K, the total value of the rate constants k_2–k_4 is 7.20×10^{-6} s^{-1}, which is 11.4 times less than $k_1 = 8.19 \times 10^{-5}$ s^{-1}.

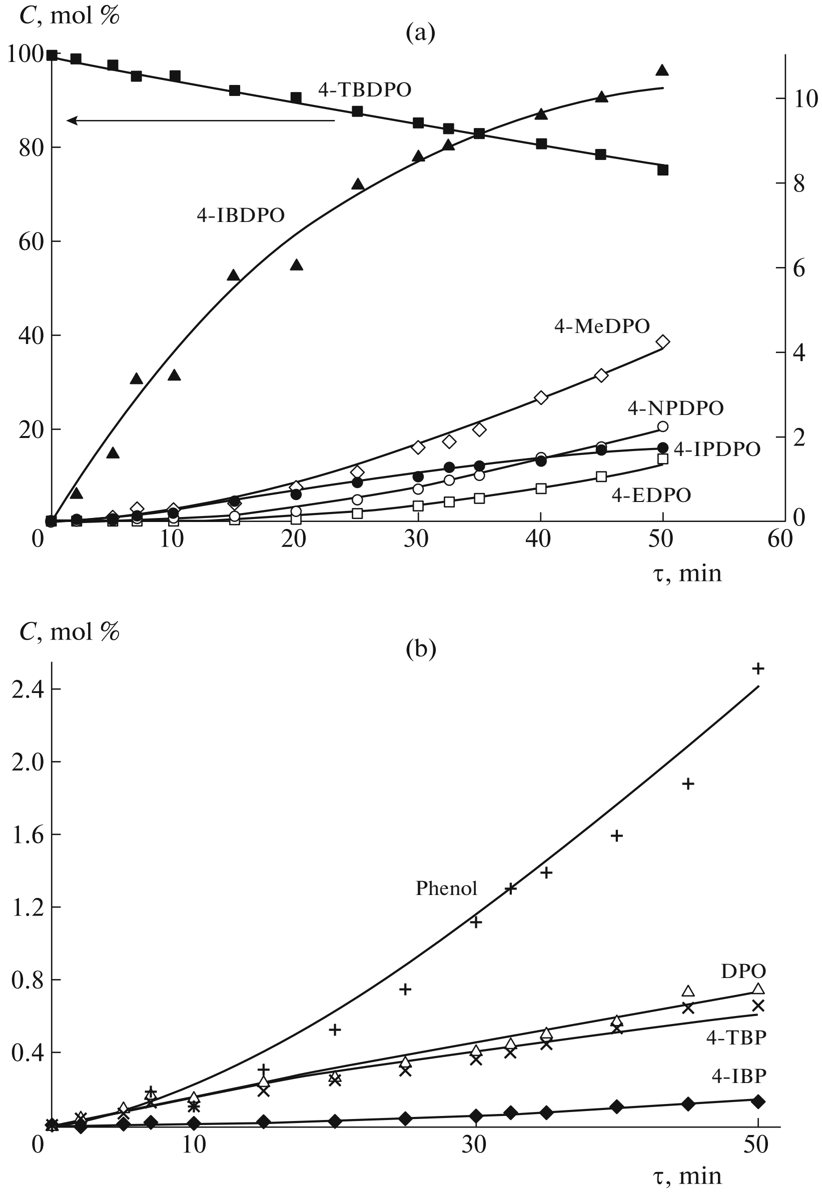

Fig. 4. Comparison of experimental (markers) and calculated (lines) concentrations of the products of thermal transformations of 4-TBDPO at 728 K: (a) (■) 4-TBDPO, (▲) 4-IBDPO, (●) 4-IPDPO, (○) 4-NPDPO, (□) 4-EDPO, (◇) 4-MeDPO; (b) (+) phenol, (△) DPO, (×) 4-TBP, (◆) 4-IBP.

In addition, it should be noted that the rate constant for the conversion 4-TBDPO → 4-IPDPO in all calculations tended to zero. According to our model, the source of 4-IPDPO and 4-MeDPO is 4-IBDPO, which undergoes active decomposition of the alkyl substituent (at 728 K, $k_5 = 2.52 \times 10^{-4}$ and $k_6 = 1.98 \times 10^{-4}$ s^{-1}).

The results of the model description of the composition of the reaction mass of the 4-TBDPO thermolysis at 728 K are presented in Fig. 4.

Calculation of Parameters of the Arrhenius Equation

The kinetic analysis of the experimental data in the range 703–763 K was performed for the reaction 4-TBDPO → products according to the equations for calculating the first-order rate constant. By linearizing the Arrhenius equation in the coordinates "lnk_i–1000/T", it was found that $k_0 = 10^{14.3 \pm 0.5}$, $E_a = 255.2 \pm 6.8$ kJ/mol. The values of the decay rate constants of 4-TBDPO are given in Table 4.

Table 4. Values of rate constants for the reaction 4-TBDPO → products proceeding during thermolysis of 4-TBDPO in the range 703–763 K

T, K	$1000/T$	k_i, s^{-1}	$-\ln(k_i)$
703	1.42	2.33×10^{-5}	10.665
708	1.41	3.56×10^{-5}	10.243
713	1.40	4.55×10^{-5}	9.998
718	1.39	5.53×10^{-5}	9.803
723	1.38	6.59×10^{-5}	9.627
728	1.37	9.03×10^{-5}	9.312
733	1.36	1.55×10^{-4}	8.770
738	1.36	2.05×10^{-4}	8.493
743	1.35	2.24×10^{-4}	8.402
748	1.34	3.48×10^{-4}	7.962
753	1.33	3.88×10^{-4}	7.855
758	1.32	5.84×10^{-4}	7.445
763	1.31	7.38×10^{-4}	7.211

For the reactions included in the kinetic model of the process in the temperature range 703–763 K, the rate constants and parameters of the Arrhenius equation were calculated. The data are given in Table 5.

CONCLUSIONS

In summary, it was found that during the thermolysis of 4-*tert*-butyl diphenyl oxide, the main conversion is the isomerization to 4-isobutyl diphenyl oxide. The mechanism of this reaction has been proposed.

In the temperature range 703–763 K, the parameters of the Arrhenius equation have been calculated for the reaction 4-TBDPO → products, namely, the preexponential factor $k_0 = 10^{14.3 \pm 0.5}$ and the activation energy $E_a = 255.2 \pm 6.8$ kJ/mol.

A kinetic model of the process has been proposed, according to which 4-IBDPO is the main source of the decay products in the temperature range of the study, namely 4-MeDPO, phenol, and 4-IPDPO. In this case, 4-NPDPO is formed by isomerization of 4-IPDPO, while 4-EDPO is the product of the destruction of these two components. The destruction of the initial 4-TBDPO proceeds to a small extent and is expressed in the breaking of the C_{Ar}–O and C_{Ar}–C_{quater} bonds to form DPO, 4-TBP, and phenol.

The information obtained can be used in the development of promising thermostable and heat-resistant polymer compositions, since it suggests the behavior of their structure at elevated temperatures. The revealed regularities, in general, can serve as the basis for further studies of the thermal stability of compounds of the class of alkyl diphenyl oxides.

Table 5. Values of parameters of the Arrhenius equation for transformations accompanying thermolysis of 4-TBDPO in the range 703–763 K

Reaction		k_i	$\log k_0$	E_a, kJ/mol	R
4-TBDPO	4-IBDPO	k_1	13.8 ± 0.5	248.6 ± 7.0	0.99
4-TBDPO	DPO	k_2	15.1 ± 0.7	286.6 ± 9.5	0.98
4-TBDPO	Phenol	k_3	15.1 ± 0.6	289.4 ± 8.1	0.99
4-TBDPO	4-TBP	k_4	14.3 ± 0.5	276.6 ± 7.3	0.99
4-IBDPO	4-IPDPO	k_5	15.7 ± 0.6	267.3 ± 9.0	0.98
4-IBDPO	4-MeDPO	k_6	14.9 ± 0.6	257.7 ± 7.7	0.99
4-IBDPO	Phenol	k_7	15.3 ± 0.4	268.0 ± 5.7	0.99
4-IPDPO	4-NPDPO	k_8	12.6 ± 0.3	218.0 ± 4.7	0.99
4-IPDPO	4-EDPO	k_9	15.3 ± 0.4	264.0 ± 5.5	0.99
4-NPDPO	4-EDPO	k_{10}	14.3 ± 0.6	247.7 ± 9.1	0.99
4-TBP	4-IBP	k_{11}	12.5 ± 0.5	228.3 ± 6.6	0.99

REFERENCES

1. D. Cabaleiro, M. J. Pastoriza-Gallego, M. M. Piñeiro, et al., J. Chem. Thermodyn. **50**, 80 (2012).
2. D. Cabaleiro, J. J. Segovia, M. C. Martin, et al., J. Chem. Thermodyn. **93**, 86 (2016).
3. J. C. Che, J. A. Wu, S. W. Li, et al., React. Funct. Polym. **78**, 23 (2014).
4. W. Q. Hu, Z. K. Cui, J. Jin, et al., Appl. Surf. Sci. **258**, 507 (2011).
5. E. S. Blake, C. W. Hammann, J. W. Edwards, et al., J. Chem. Eng. Data **6**, 87 (1961).
6. M. T. Jackson, Jr. and J. Q. Walker, J. Anal. Chem. **43**, 74 (1971).
7. M. Laatikainen, K. Vahteristo, S. Saukkonen, et al., Ind. Eng. Chem. Res. **35**, 2103 (1996).
8. H. J. Ederer, A. Kruse, C. Mas, et al., J. Supercrit. Fluids **15**, 191 (1999).
9. J. Yu and S. Eser, Ind. Eng. Chem. Res. **37**, 4591 (1998).
10. L. N. C. Guerra, L. J. C. Huerta, C. Lorgeoux, et al., J. Anal. Appl. Pyrolys. **133**, 234 (2017).
11. K.-U. Buhler, *Spezialplaste* (Akademie, Berlin, 1978).
12. A. I. Druzhinina, S. M. Pimenova, S. V. Tarazanov, et al., J. Chem. Thermodyn. **87**, 69 (2015).
13. V. A. Shakun, T. N. Nesterova, and S. V. Tarazanov, Pet. Chem. **59**, 120 (2019).
14. A. T. Lebedev, *Mass Spectrometry in Organic Chemistry* (Binom, Moscow, 2003) [in Russian].
15. E. Pretsch, P. Buhlmann, and C. Affolter, *Structure Determination of Organic Compounds: Tables of Spectral Data* (Springer, 2000).
16. http://webbook.nist.gov/.
17. P. J. Robinson and K. A. Holbrook, *Unimolecular Reactions* (Wiley, London, 1972).

Translated by V. Avdeeva